

## LEARNING ABOUT JET PHYSICS FROM GAMMA-RAY BLAZARS

M. Sikora, R. Moderski, N. Copernicus Astron. Ctr., Warsaw, Poland;  
G. Madejski, NASA/Goddard, USA; J. Poutanen, Stockholm Observatory, Sweden

## ABSTRACT

We use spectral properties of the MeV-radiation dominated blazars to put constraints on physical parameters of relativistic jets in *quasars*. Specifically, using the luminosities and positions of high energy and low energy spectral components, we derive constraints on the jet speeds, magnetic fields, and the distances at which most of nonthermal radiation is produced. By comparing the theoretically predicted bulk-Compton radiation with the observed soft X-ray luminosities, we find upper limits on the optical thickness, and lower limits on the distance where the relativistic jet is formed and collimated.

Our results show that these jets should be Thomson optically thin and, in the case of  $\gamma$ -ray production dominated by the ERC (External-Radiation-Compton) process, favor proton-electron jets. Much weaker constraints on the pair plasma content are provided if the  $\gamma$ -ray production is dominated by the SSC (Synchrotron Self-Compton) process. However, the SSC models predict too small jet Lorentz factors  $\Gamma_j$  ( $\sim 3$ ) as compared with those observed by VLBI in quasars ( $\sim 10$ ), and require jets to be very weakly magnetized.

Keywords: quasars; high energy astrophysics; gamma-rays;

## 1. INTRODUCTION

Typical spectrum of a  $\gamma$ -ray blazar consists of two components (cf. Fig. 1), the low energy one (LE) peaking at IR-optical wavelengths, and the high energy one (HE) which in many quasar-hosted blazars peaks at MeV energies (see, e.g., von Montigny et al. 1995). The high polarization, large amplitude of variability, and the non-thermal shape imply that the LE-component is most likely due to emission via the synchrotron process from a jet pointing closely to the line of sight (Blandford & Rees 1978). The HE-component, on the other hand, is most likely due to the inverse-Compton process by the same electrons that produce the synchrotron photons. The seed photons for the inverse-Compton process can be provided by synchrotron radiation in the jet and/or by radiation from the central source, scattered or reprocessed by the broad emission line clouds and intercloud medium.

The most extreme blazars are those dominated by MeV radiation, and so far, these are always observed to be hosted in quasars. We use the spectral properties of these objects to derive physical parameters of their jets. Specifically: from the ratio of the peak luminosities, we derive constraints on ratio of the Poynting flux to the kinetic energy flux and on jet Lorentz factors (§2); from location of the spectral peaks we derive distance in a jet at which the peaks are produced (§3); and from the deficit of flux in the X-ray regime, we derive upper limits on the optical thickness and the pair content of a jet plasma (§4). Our analysis is performed separately for two extreme cases: where the  $\gamma$ -ray production is strongly dominated by Comptonization of synchrotron radiation (the SSC models: Rees 1967; Königl 1981; Marscher & Gear 1985; Ghisellini & Maraschi 1989), and where  $\gamma$ -rays result mostly from Comptonization of external radiation (the ERC models: Dermer & Schlickeiser 1993; Sikora, Begelman, & Rees 1994; Blandford & Levinson 1995; Ghisellini & Madau 1996). Our results are summarized in §5.

## 2. LUMINOSITIES OF THE HE- AND THE LE-PEAK

We assume that jet is steady-state, and has conical geometry with the opening half-angle  $\theta_j \geq 1/\Gamma_j$ . We also assume that: both the LE and the HE spectral peaks are produced in the same jet region and by the same electrons; pair cascades are not involved; and the change of the spectral slope around the peaks results from the break in the electron injection spectrum (a homogeneous case), or from superposition of partial spectra produced over wider range of distances (an inhomogeneous case). Since our analysis is based only on the values of luminosities at the spectral peaks, our results will be the same for both cases.

## 2.1. ERC process vs. SSC process

In the comoving frame of a jet, energy densities of synchrotron radiation and external radiation are

$$u'_S \sim \frac{L_S}{4\pi r^2 c \Gamma_j^2}, \quad (1)$$

$$u'_D \sim \frac{\xi L_{UV} \Gamma_j^2}{4\pi r^2 c}, \quad (2)$$

respectively, where  $\xi$  is the fraction of the central source UV radiation being isotropized at a distance  $r$  due to reprocessing by broad emission line clouds and intercloud medium (Sikora et al. 1994; 1996), and  $L_S$  is the observed synchrotron luminosity.

Since Compton energy losses of relativistic electrons in SSC and ERC processes scale respectively with  $u'_S$  and  $u'_D$ , eqs. (1) and (2) imply that the production of  $\gamma$ -rays in blazars is dominated by the SSC process rather than by ERC process, only if  $\Gamma_j < \Gamma_0$ , where

$$\Gamma_0 \simeq \left( \frac{L_S}{\xi L_{UV}} \right)^{1/4} \simeq 3 \left( \frac{L_{S,47}}{(\xi L_{UV})_{45}} \right)^{1/4}, \quad (3)$$

where  $L_{S,47} = L_S/10^{47}$  ergs s<sup>-1</sup>, and  $(\xi L_{UV})_{45} = \xi L_{UV}/10^{45}$  ergs s<sup>-1</sup>.

## 2.2. The case of the SSC process domination

Magnetic energy density, as measured in the jet co-moving frame is

$$u'_B \sim \frac{L_B}{\Omega_j r^2 c \Gamma_j^2}, \quad (4)$$

where  $\Omega_j = \pi \theta_j^2$  is the jet solid angle, and  $L_B$  is the Poynting flux. Then the ratio of SSC luminosity to synchrotron luminosity (both dominated at peaks) is

$$\frac{L_{SSC}}{L_S} \sim \frac{u'_S}{u'_B} \sim \frac{\Omega_j L_S}{4\pi L_B}. \quad (5)$$

Noting that for the SSC model  $L_{SSC} \gg L_{ERC}$ , we find that for  $\gamma$ -ray dominated blazars ( $\rightarrow L_{SSC} \gg L_S$ ), the luminosity of injected relativistic electrons is

$$L_{inj} \simeq L_{SSC,em} \simeq \frac{\Omega_j}{4\pi} L_{SSC}. \quad (6)$$

Combining eqs. (5) and (6), we have the fraction of the total jet power that is contributed by the Poynting flux

$$\epsilon_B \equiv \frac{L_B}{L_j} \simeq \epsilon_{inj} \left( \frac{L_S}{L_{SSC}} \right)^2, \quad (7)$$

where  $\epsilon_{inj} = L_{inj}/L_j$ ,  $L_j = L_B + L_K$  is the total jet power, and  $L_K$  is the kinetic energy flux. Since from energy conservation  $L_{inj} < L_j$ , eq. (7) implies that high ratios  $L_{SSC}/L_S$  can be achieved only for very weakly magnetized jets.

## 2.3. The case of the ERC process domination

In the case of the ERC models  $L_{ERC} \gg L_{SSC}$ , and for  $\gamma$ -ray dominated spectra ( $\rightarrow L_{ERC} \gg L_S$ )

$$L_{inj} \simeq \frac{\Omega_j}{4\pi} L_{ERC}. \quad (8)$$

Combining this with

$$\frac{L_{ERC}}{L_S} \sim \frac{u'_D}{u'_B} = \frac{\Omega_j \xi L_{UV} \Gamma_j^4}{4\pi L_B}, \quad (9)$$

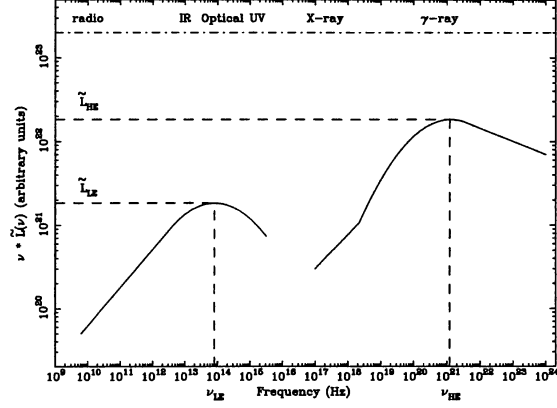


Figure 1: Schematic representation of a broad-band spectrum of a MeV-dominated blazar

gives

$$\Gamma_j \simeq \left( \frac{\epsilon_B}{\epsilon_{inj}} \frac{L_{ERC}^2}{\xi L_{UV} L_S} \right)^{1/4} \simeq 10 \left( \frac{\epsilon_B}{\epsilon_{inj}} \frac{L_{ERC,48}^2}{(\xi L_{UV})_{45} L_{S,47}} \right)^{1/4}, \quad (10)$$

where  $L_{ERC,48} = L_{ERC}/10^{48}$  ergs s<sup>-1</sup>. Thus, the high ratio of the  $\gamma$ -ray luminosity to other spectral components can be reproduced by ERC models if  $\Gamma_j \sim 10$ .

Note, however, that for  $\Gamma_j$  given by eq. (10), the domination of ERC radiation over SSC radiation ( $\Gamma_j > \Gamma_0$ ) is satisfied for any  $\epsilon_B > \epsilon_{inj} (L_S/L_{ERC})^2$ , and that for  $\epsilon_B$  approaching the lower limit, the required  $\Gamma_j$  can be as small as  $\Gamma_0$  given by eq. (3).

## 3. LOCATIONS OF HE- AND LE-PEAK

### 3.1. The case of the SSC process domination

Let us denote the location of luminosity peaks in the observed spectrum by  $x_{LE}$  and  $x_{HE}$ , where  $x \equiv h\nu/m_e c^2$  (cf. Fig. 1). Then, in the SSC model  $x_{LE} = \Gamma_j x'_S$  and  $x_{HE} = \Gamma_j x'_{SSC}$ , where  $x'_S$  and  $x'_{SSC}$  are energies of synchrotron and SSC photons, respectively, produced by electrons with injection function break-energy,  $\gamma'_m$  (note that in case of an inhomogeneous model this break-energy can correspond with the maximum electron energies as produced in the region where the luminosity peaks originate). Using approximate formulae for photon energies produced by synchrotron and SSC processes in the jet co-moving frame,

$$x'_S \simeq \gamma'_m{}^2 (B'/B_{cr}), \quad (11)$$

and

$$x'_{SSC} \simeq \gamma'_m{}^2 x'_S, \quad (12)$$

where  $B_{cr} \equiv m_e^2 c^3 / \hbar e \simeq 4.4 \times 10^{13}$  G, we obtain

$$\gamma'_m \simeq \sqrt{\frac{x'_{SSC}}{x'_S}} \simeq 3 \times 10^3 \sqrt{\frac{x_{HE}/10}{x_{LE}/10^{-6}}}, \quad (13)$$

and

$$B' \simeq \frac{x'_S}{\gamma'_{max}} B_{cr} \simeq \frac{1}{(\Gamma_j/3)} \frac{(x_{LE}/10^{-6})^2}{x_{HE}/10} \text{ G}. \quad (14)$$

Combining eq. (14) with eqs. (4) and (5), one can find the distance at which the production of synchrotron and SSC radiation peaks,

$$\begin{aligned} r_{SSC} &\simeq \sqrt{\frac{L_B}{cu'_B \Gamma_j^2 \Omega_j}} \simeq \frac{1}{\Gamma_j B'} \sqrt{\frac{2L_S^2}{cL_{SSC}}} \\ &\simeq 2 \times 10^{17} \frac{x_{HE}/10}{(x_{LE}/10^{-6})^2} \frac{L_{S,47}}{L_{SSC,48}^{1/2}} \text{ cm}. \end{aligned} \quad (15)$$

For black hole masses  $10^8 - 10^9 M_\odot$ , this gives  $r_{SSC} \sim 10^3 - 10^4 r_g$ , where  $r_g = 2GM_{BH}/c^2$  is the gravitational radius.

### 3.2. The case of the ERC process domination

Here,  $x_{HE} = \Gamma_j x'_{ERC}$  and, as before,  $x_{LE} = \Gamma_j x'_S$ . External photons with energies  $x_{UV}$  and reaching the jet from aside have in a jet comoving frame energies  $\sim \Gamma_j x_{UV}$ , and scattered off the electrons with energies  $\gamma'_m$  reach energies

$$x'_{ERC} \simeq \gamma'_m{}^2 \Gamma_j x_{UV}. \quad (16)$$

From eq. (16)

$$\gamma'_m \simeq \sqrt{\frac{x'_{ERC}}{\Gamma_j x_{UV}}} = \frac{10^2}{(\Gamma_j/10)} \sqrt{\frac{x_{HE}/10}{x_{UV}/10^{-5}}}, \quad (17)$$

which together with eq. (11) gives

$$\begin{aligned} B' &\simeq \frac{x'_S}{\gamma'_{max}} B_{cr} \\ &\simeq 4 \times 10^2 (\Gamma_j/10) \frac{(x_{LE}/10^{-6})(x_{UV}/10^{-5})}{x_{HE}/10} \text{ G}. \end{aligned} \quad (18)$$

Now, using eqs. (18) and (9) in the formula for the Poynting flux we obtain

$$\begin{aligned} r_{ERC} &\simeq \sqrt{\frac{L_B}{cu'_B \Gamma_j^2 \Omega_j}} \\ &\simeq \frac{2 \times 10^{15} (x_{HE}/10)}{(x_{LE}/10^{-6})(x_{UV}/10^{-5})} \sqrt{\frac{(\xi L_{UV})_{45} L_{S,47}}{L_{ERC,48}}} \text{ cm}. \end{aligned} \quad (19)$$

This gives the approximate location of the region where according to the ERC model most of radiation is produced. It is about  $10 - 10^2 r_g$  from the black hole of mass  $10^8 - 10^9 M_\odot$ .

## 4. SOFT X-RAYS VS. BULK-COMPTON RADIATION PREDICTIONS

The external diffuse radiation is Comptonized not only by relativistic electrons in a jet, but also by non-relativistic electrons in a jet. The power of the radiation produced by nonrelativistic electrons enclosed within the jet volume element  $\Omega_j r^2 dr$  is

$$dL_{BC,em} \simeq m_e c^2 \left| \frac{d\Gamma_j}{dt} \right| n_e \Omega_j r^2 dr, \quad (20)$$

where  $n_e(r)$  is the number density of nonrelativistic electrons,  $|d\Gamma_j/dt| \simeq c\sigma_T u'_D/m_e c^2$ , and  $u'_D$  is given by eq. (2). Let us define  $r_{min}$  to be the distance along the jet below which the jet is assumed to be not fully developed yet, i.e. not sufficiently accelerated, collimated, or mass loaded to contribute significantly to the bulk-Compton radiation and any other beamed radiation components. Noting then that for a relativistic conical outflow  $n_e(r) \simeq n_e(r_{min}) \times (r_{min}/r)^2$ , we obtain that observer located at  $\theta_{obs} \leq \theta_j$  will see

$$L_{BC} \simeq \frac{4\pi}{\Omega_j} L_{BC,em} \simeq n_e(r_{min}) r_{min} \sigma_T \xi L_{UV} \Gamma_j^2, \quad (21)$$

peaked at

$$x_{BC} \simeq \Gamma_j^2 x_{UV} \simeq 10^{-3} (\Gamma_j/10)^2. \quad (22)$$

This is at  $\sim 1$  keV, precisely where the  $\gamma$ -ray dominated blazars show strong deficiency of radiation (see Fig. 1). As we show below, comparison of  $L_{BC}$  with observed soft X-ray luminosities,  $L_{SX}$ , provides severe constraints on jet optical thickness and on minimum distance from the central engine.

### 4.1. How optically thick are jets?

For a given distance  $r$  the optical thickness for Thomson scatterings in a jet is given by  $\tau_j \simeq n_e a \sigma_T$ , where  $a = \theta_j r$ . Using the observational constraint  $L_{BC} \leq L_{SX}$ , we find that

$$\tau_j(r_{min}) \leq \frac{L_{SX}}{\xi L_{UV}} \frac{\theta_j}{\Gamma_j^2} = 10^{-2} \frac{L_{SX,46}}{(\xi L_{UV})_{45}} \frac{10\theta_j}{(\Gamma_j/10)^2}. \quad (24)$$

Thus, highly relativistic and collimated jets must be very optically thin, or otherwise they would overproduce soft X-rays. This imposes serious constraints on any radiation models which involve such processes as pair annihilation and Coulomb interactions. This is because in such thin plasmas, the time scales of these processes are much longer than the jet propagation time scale (Dermer, Sturmer, & Schlickeiser 1996).

### 4.2. How close to the black hole are jets formed?

The optical thickness of a conical relativistic jet at any given distance can be calculated using the formula for kinetic power. In the case of jet inertia dominated by cold protons, this power is given by

$$L_K \simeq n_p m_p c^3 \Omega_j r^2 \Gamma_j. \quad (24)$$

Combining this with the definition of  $\tau_j$ , we obtain

$$\tau_j \simeq \frac{\theta_j}{\Gamma_j} \frac{4\pi n_e}{\Omega_j n_p} \frac{L_K}{L_{Edd}} \frac{r_g}{r}, \quad (25)$$

where  $L_{Edd} = (4\pi m_p c^3 / \sigma_T) r_g$ . Using eqs. (23) and (25), and relation

$$L_K = (1 - \epsilon_B) L_j = \frac{1 - \epsilon_B}{\epsilon_{inj}} L_{inj} \simeq \frac{1 - \epsilon_B}{\epsilon_{inj}} \frac{\Omega_j}{4\pi} L_\gamma, \quad (26)$$

one can find that overproduction of soft X-rays can be avoided only if

$$\begin{aligned} \frac{r_{min}}{r_g} &\geq \frac{4\pi n_e}{\Omega_j n_p} \frac{L_K}{L_{Edd}} \frac{\xi L_{UV}}{L_{SX}} \Gamma_j \\ &\simeq 10 \frac{1 - \epsilon_B}{\epsilon_{inj}} \frac{n_e}{n_p} \frac{(\xi L_{UV})_{45}}{L_{Edd,47}} \frac{L_{\gamma,48}}{L_{SX,46}} \frac{\Gamma_j}{10}, \end{aligned} \quad (27)$$

where  $L_\gamma = L_{ERC} + L_{SSC}$ . Thus, as one can see from eq. (27), for strongly pair dominated jets, the value of  $r_{min}$  as high as  $10^4 r_g$  is required in order to avoid soft X-ray radiation above the observed levels. (Note that for  $n_e > n_p m_p / m_e$  the term  $n_p m_p$  in the formula (24) must be replaced by  $n_e m_e$ , and then the term  $n_e / n_p$  in eqs. (25) and (26) ought to be replaced by  $m_p / m_e$ .)

#### 4.3. Pair content

For any model attempting to explain the large  $\gamma$ -ray luminosities in terms of relativistic beaming, most of  $\gamma$ -rays must be produced at distances  $\geq r_{min}$ . In the case of an inhomogeneous SSC model, this implies  $r_{SSC} \geq r_{min}$ , and using eqs. (15) and (27) we obtain

$$\begin{aligned} \frac{n_e}{n_p} &< \frac{\epsilon_{inj}}{1 - \epsilon_B} \frac{L_{Edd}}{\xi L_{UV}} \frac{L_{SX}}{L_{SSC}} \frac{1}{\Gamma_j} \frac{r_{SSC}}{r_g} \\ &\simeq 10^2 \frac{\epsilon_{inj}}{1 - \epsilon_B} \frac{x_{HE} / \Gamma_j}{(x_{LE} / 10^{-6})^2} \frac{L_{SX,46} L_{S,47}}{(\xi L_{UV})_{45} L_{SSC,48}^{3/2}}. \end{aligned} \quad (28)$$

This shows that in the SSC model, the overproduction of soft X-rays due to bulk-Compton process can be serious only for highly pair-dominated jets.

In the case of the ERC model (inhomogeneous version without pair production), the condition  $r_{ERC} \geq r_{min}$  combined with equations (19) and (27) gives

$$\begin{aligned} \frac{n_e}{n_p} &\leq \frac{\epsilon_{inj}}{1 - \epsilon_B} \frac{L_{Edd}}{\xi L_{UV}} \frac{L_{SX}}{L_{ERC}} \frac{1}{\Gamma_j} \frac{r_{ERC}}{r_g} \\ &\simeq \frac{\epsilon_{inj}}{1 - \epsilon_B} \frac{x_{HE} / \Gamma_j}{(x_{LE} / 10^{-6}) (x_{UV} / 10^{-5})} \frac{L_{SX,46} L_{S,47}^{1/2}}{(\xi L_{UV})_{45}^{1/2} L_{ERC,48}^{3/2}}. \end{aligned} \quad (29)$$

This implies that the pair content of a jet is more severely limited in the ERC models than in the SSC models. The reason for this is that  $r_{min}$  limited by  $r_{ERC}$  is  $\sim 100$  lower than  $r_{min}$  limited by  $r_{SSC}$  (compare eqs. [15] and [19]).

## 5. CONCLUSIONS

Using the spectral properties of MeV-radiation dominated blazars, we derived the following constraints on SSC and ERC models:

- The very high ratio of peak luminosities,  $L_\gamma / L_S > 10$ , can be reproduced by the SSC models only for very weakly magnetized jets,  $\epsilon_B < 0.01$  (see eq. [7]), and modest jet Lorentz factors,  $\Gamma_j \leq 3$  (see eq. [3]);
- If production of the synchrotron and Compton luminosity peaks is dominated by the same population of electrons and with this same energy range, then observed location of high energy and low energy peak implies the production of  $\gamma$ -rays by ERC models very close to the black hole (see eq. [19]);
- All jet models with pair dominated plasmas – unless the jet develops fully (i.e. is accelerated, collimated and matter loaded) beyond  $r \sim 10^4 r_g$  – predict large radiation excesses to be produced by Comptonization of external radiation by cold electrons in a jet. These, expected to be observed as soft X-ray excesses at  $\sim 1$  keV, have not been confirmed by observations so far.

ACKNOWLEDGMENTS: We would like to acknowledge support from ITP and JILA where part of this work has been accomplished. The research was supported by NASA grant NAG5-2026, and the Polish KBN grants 2P03D01209 and 2P03D01010.

## REFERENCES

- Blandford, R. D., & Rees, M. J. 1978, in Pittsburgh Conference on BL Lac Objects, ed. A. N. Wolfe (Pittsburgh University Press), 328
- Blandford, R. D., & Levinson, A. 1995, ApJ, 441, 79
- Dermer, C. D., & Schlickeiser, R. 1993, ApJ, 416, 458
- Dermer, C. D., Sturmer, S. J., & Schlickeiser, R. 1996, ApJ, submitted
- Ghisellini, G., & Madau, P. 1996, MNRAS, 280, 67
- Ghisellini, G., & Maraschi, L. 1989, ApJ, 340, 181
- Königl, A. 1981, ApJ, 243, 700
- Marscher, A., & Gear, W. 1985, ApJ, 198, 114
- Rees, M. 1967, MNRAS, 137, 429
- Sikora, M., Begelman, M. C., & Rees, M. J. 1994, ApJ, 421, 153
- Sikora, M., Sol, H., Begelman, M. C., & Madejski, G. M. 1996, MNRAS, 280, 781
- von Montigny, C., et al. 1995, ApJ, 440, 525